

Control Strategies for High Frequency Voltage Source Converter for Ozone Generation

Jakson P. Bonaldo and José A. Pomilio
University of Campinas – Campinas – Brazil

jbonaldo@gmail.com, antenor@dsce.fee.unicamp.br

Abstract-This paper presents a resonant converter for ozone generation developed for corona discharge processes. The switching frequency is adjusted near the series resonance between the leakage inductance of transformer and the equivalent capacitance of the ozone generation cell, allowing high efficiency, due to high power factor and power switches soft-switching. Power regulation is provided by Pulse Density Modulation – PDM. As the converter is a voltage source inverter it is necessary to limit the instantaneous current and its average value in order to avoid the saturation of the high-voltage transformer. Simulation and experimental results show the behavior of the proposed circuit and controller.

I. INTRODUCTION

Due to the biocide characteristic and low average time life, ozone becomes interesting for applications like sterilization of surgical equipments, water and effluents treatment from industrial processes.

The industrial generation of ozone is carried out by high voltage electrical discharges between two electrodes, breaking down the oxygen molecule O_2 , which recombines in ozone, O_3 [1]. The oxygen flows between two electrodes in which the electrostatic discharge occurs. In typical ozonizer cells there is a dielectric material, usually glass and an air gap.

To supply the high voltage necessary to break down the air dielectric, it is used a transformer with high turns ratio. The use of high frequency is convenient for increasing the discharges and, consequently, the ozone production. Such transformers, due to the secondary side turns and isolation requirements, typically present high values of leakage inductance and parallel capacitance, which produce a series resonance in relatively low frequency. Next to this resonance the voltage gain becomes higher than the turns ratio, boosting the discharging process. Additionally, from the converter point of view, operating next to the resonance allows soft-commutation, what improves the converter efficiency.

There are many papers available about power supplies for ozone generators [2-4]. Some of these works concerns the regulation of the load power. Typically, the transformer saturation is avoided by using current fed converters, what means it is necessary an addition converter for regulating the input current. In [5] the saturation control is based on Pulse Density Modulation – PDM. The use of this implementation

with other modulation technique, like frequency modulation, is not discussed.

The use of a voltage source converter has the advantage of eliminating the input converter necessary for current regulation, however, it is necessary an active current control to avoid the saturation of the transformer. This work presents a method for current limitation applicable to voltage sources topologies and useful with any modulation technique.

II. SYSTEM MODEL

For system modeling it is necessary to obtain the parameter of the high frequency high voltage transformer, as well as the model of ozone generation cell.

A. Ozone Generation Cell Model

Two models used for the electrostatic cell are shown in Fig. 1. The more complete model for the cell, shown in Fig. 1.a, divides the capacitance of the air gap and capacitance of the glass, C_a and C_v , respectively. The voltage V_z corresponds to the level of the electrostatic discharge and also is the element that consumes power. For modeling purposes, during the discharge, the diodes maintain the voltage on C_a , increasing the total capacitance seen by the source to the value of C_v [2].

A simple linear model [6] is shown in Fig. 1.b. The capacitor C_z models an average capacitance, while the resistor R_z adjusts the power demanded by the cell.

The models parameters values can be calculated from the cell dimensions (first model); measured in low voltage (what gives the equivalent value of the series association of C_a and C_v) or, for the second model, estimated in the real operation [6].

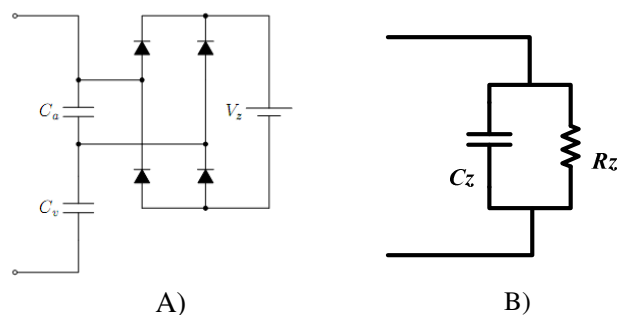


Fig. 1 - Models for ozone generation cell. A) Detailed non-linear model; B) Simplified linear model

B. Model of High Voltage Transformer

Transformers of high frequency and high voltage are better modeled if including some parameters usually not considered for low-frequency, low-voltage transformers. The capacitances, usually neglected in models in low frequency and voltage, have greater influence and, therefore, must be considered.

Fig. 2. shows a simplified model with lumped parameters for high frequency high voltage transformers. Where:

- R_s – equivalent windings resistance;
- L_d – leakage inductance;
- R_p – resistance associated to the core losses;
- C_p – windings capacitance;
- L_m – magnetizing inductance;
- n – turns ratio

The capacitance between windings is neglected, since its influence is beyond the frequency range of interest for the application. The secondary side winding capacitance has a major influence. When referred to the primary side, it is multiplied by the square of the turns-ratio, making its equivalent value even more determinant of the device operation.

Figure 2.b includes the ozonizer cell (linear model) connected to the secondary. The load capacitance is added to the secondary winding capacitance. Thus, the total equivalent capacitance is called C_{eq} . Resistance R_z , when referred to the primary, is divided by the square of the turns-ratio. This resistance is lower than R_p and determines the transformer power consumption.

The parallel resonance frequency f_p between the magnetizing inductance and equivalent capacitance is given by (1). The series resonance frequency, f_s , between the leakage inductance and the equivalent capacitance is given by (2).

$$f_p = \frac{1}{2\pi\sqrt{L_m C_{eq}}} \quad (1)$$

$$f_s = \frac{1}{2\pi\sqrt{L_d C_{eq}}} \quad (2)$$

$$Z_{in} = \frac{R_s + s \left[L_d + L_m \left(1 + \frac{R_s}{R_{pe}} \right) \right] + s^2 L_m \left(\frac{L_d}{R_{pe}} + C_{eq} R_s \right) + s^3 L_d L_m C_{eq}}{1 + s \frac{L_m}{R_{pe}} + s^2 L_m C_{eq}} \quad (3)$$

$$\frac{V_o}{V_{inv}} = n \cdot \frac{s R_p L_{mag}}{s^3 R_{pe} L_d L_m C_{eq} + s^2 (R_s R_{pe} L_m C_{eq} L_d L_m) + s (R_s L_m + R_{pe} L_d + R_{pe} L_m) + R_s \cdot R_{pe}} \quad (4)$$

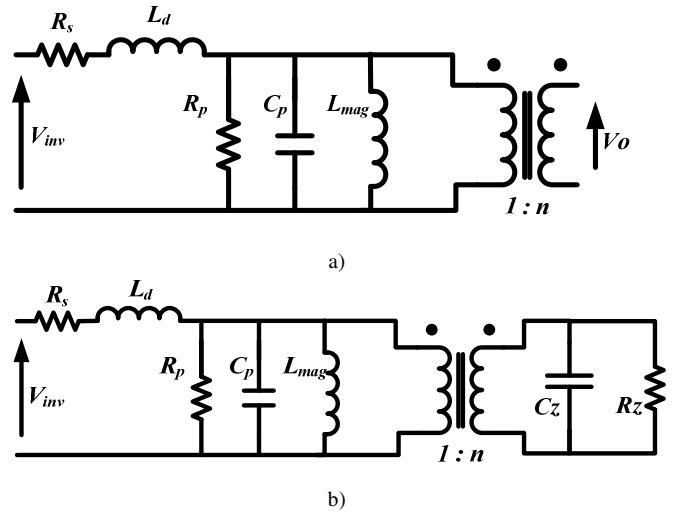


Fig. 2. a) Transformer simplified model; b) Ozone generation cell connected to the transformer

The input impedance of the transformer plus the ozone generating cell is given by (3). The transfer function of the system, which expresses the relationship between the input and output voltage is shown in (4). Parameter R_{pe} represents the association of R_p with R_z .

C. Transformer Parameters Determination

To determine the transformer parameters, it is used the method proposed in [7]. Two considerations must be recognized: the leakage inductance must be significantly smaller than the magnetizing inductance and the frequency at which the measures are taken, should be low enough in order to make the capacitance between the windings negligible.

Measuring then the inductance of the transformer primary with the secondary open, one gets the magnetizing inductance plus the leakage inductance. This value can be taken as the approximate value of the magnetizing inductance L_m .

To obtain the value of the capacitance C_p and the leakage inductance L_d it is necessary to obtain the frequencies of series and parallel resonance. These can be get scanning the frequency of the transformer with the secondary open. C_p can be obtained by replacing in (1) parameter L_m and parallel resonance frequency f_p observed. To determine the leakage inductance, just replace the series resonance frequency f_s and the observed capacitance C_p . In such test, as the applied voltage is low, there are no electrostatic discharges, the effective load capacitance is the association of C_v and C_a .

III. PULSE DENSITY MODULATION

Most of the control techniques used to adjust the output power of series resonant converters is based on frequency or DC bus voltage control. Both of them, for reducing the output power, decrease the load voltage. However, to get electrostatic discharge, it is necessary to reach a minimum voltage on the ozonizer cell. If the voltage is lower than the required value, the ozone production goes to zero or, it creates partial discharge due to non-uniformity of air gap between the glass and the electrode of the cell.

Figure 3 shows the steps of operation for the converter running at PDM. The load corresponds to a series LC circuit and the load is connected in parallel with the capacitance.

The switching frequency is above the series resonance. In this range, the transistors turn-on is soft since, in the inductive region, the current lags the voltage. The anti-parallel diode conducts before the respective transistor, performing zero-current commutation. For the turn-off, the switch capacitances (or additional capacitors connected between emitter and collector) realize a zero-voltage commutation.

The inverter synthesizes a square wave during operation alternating between modes I and II. During the operation mode III, the lower switches of the inverter bridge are kept on, forming a bidirectional free-wheeling path, allowing the free flow of current while the voltage across the load is zero. This period is also known as free resonance. The voltage and current waveforms resulting from this process can be viewed in Figure 4.

Adjusting the density of voltage pulses can regulate the average output power of the inverter. Figure 4 corresponds to the case of a pulse density of 5/8. Since the modes I and II are alternated for five cycles. After the fifth cycle, the inverter goes to mode III for the remaining three cycles. The load current suffers a damping, which depends on the quality factor of the load (intended as transformer plus ozonizer cell). For this case, the average power is 5/8 of the maximum power obtained with unitary pulse density.

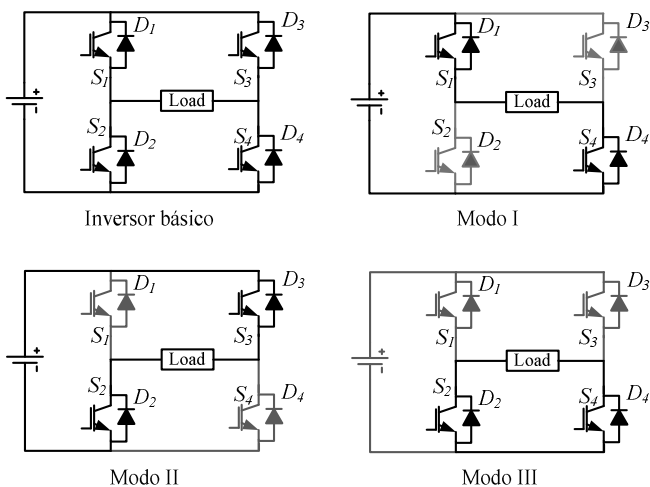


Fig. 3. State of the switches operating in PDM.

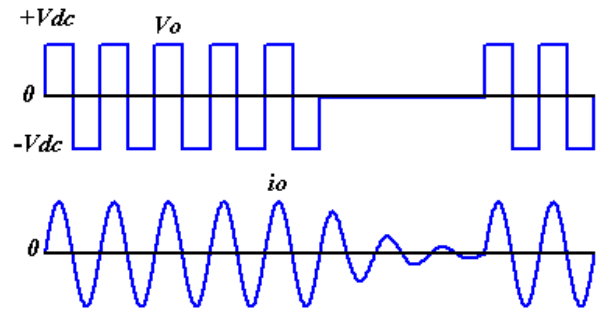


Fig. 4. Standard switching operation in PDM.

IV. CONTROL OF TRANSFORMER SATURARION

The general scheme of the proposed anti-saturation control can be seen in Fig. 5. The current limiter block represents the fast current control. The PI block represents the proportional+integral controller, used to bring the average level of the transformer input voltage to zero. The average current is obtained by filtering the current. K is the sensor gain used in signal acquisition. The average current is compared with the reference to generate the error current that enters the PI controller. For steady-state the desired average current is zero. The PI generates the reference for the pulse width modulator. In the modulator, the reference supplied by PI is compared with a triangle wave to produce the pulses that activate the power switches. In normal operation the pulse-width corresponds to half-cycle. However, if the circuit detects over-current, it is cut-down before the end of the half-cycle.

A. Fast Current Control

In the current control circuit, the pulse width modulator generates the signals represented by g in Fig. 6. Before being applied to the inverter switches, these pulses are modulated by current control unit, which applies full or partial pulses to the switches, depending on the instantaneous value of load current.

If the current hit the levels indicated by *Upper* and *Lower*, the command pulses are blocked, preventing the voltage from reaching a magnitude that could endanger the safe operation of the system due to transformer saturation or any other overcurrent phenomena.

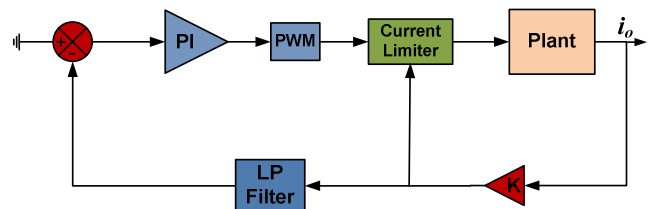


Fig. 5. General scheme of the proposed anti-saturation control

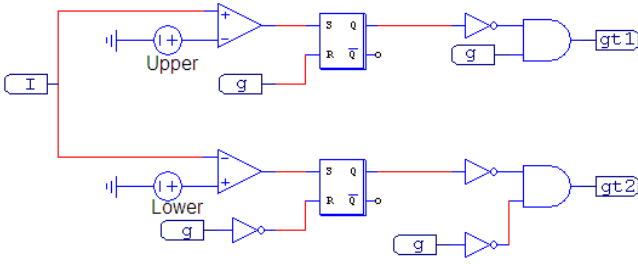


Fig. 6. Current control circuit.

In the subsequent cycle, the load current may reach the limits again, causing the application of another incomplete pulse. It may generate an average level in the inverter output voltage, causing the saturation of the transformer and influencing the amount of average power delivered to the cell.

Figure 7 shows the waveforms concerning the operation of the current control circuit. Note the interruptions in the pulses, leading to an average level in voltage and current. This limitation of the instantaneous current control justifies the inclusion of proportional integral controller.

The method used for tuning and implementation is presented in the following sections

B. Average voltage control

The function of the integral action is to eliminate the steady state error of the average current. The error signal $e(t)$ is multiplied by a proportional gain K_p , combined with the integral of the error, performed with time constant T_i , as shown in (5). The transfer function of PI controller is modeled in (6).

$$u(t) = K_p \left[e(t) + \frac{1}{T_i} \int e(t) \right] \quad (5)$$

$$G_{PI}(s) = K_p + \frac{K_I}{s} \quad (6)$$

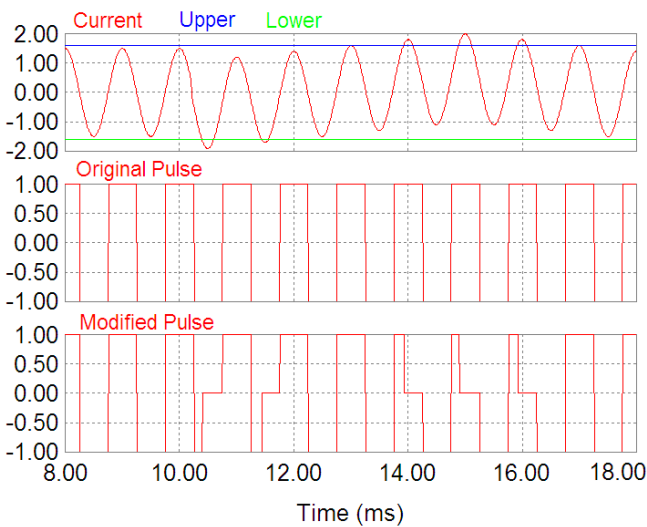


Fig. 7. Waveforms of the current control circuit.

The tuning of the PI is performed using the traditional method of tuning in closed loop, proposed by Ziegler and Nichols [9]. The method is based on elimination of the integral part followed by a systematical increasing of the proportional gain until the system begin to oscillate with the critical gain K_{CR} , then it is measured the period of oscillation P_{CR} . The constants are calculated with (7) and (8).

$$K_p = 0.45 K_{CR} \quad (7)$$

$$T_i = \frac{1}{1.2} P_{CR} \quad (8)$$

As the method does not provide an optimal response, the results were taken as reference, until it reach the values of $K_p = 0.5$ and $T_i = 0.04$.

The PI controller is implemented in a digital processor, so it is necessary to discretize, as shown in (9). Where $u_p[n]$ corresponds to the proportional output and $u_i[n]$ corresponds to the integral output [10]. The output of the controller proportional+integral corresponds to $u[n]$.

$$\begin{aligned} u[n] &= u_p + u_i \\ u_p[n] &= K_p \cdot e[n] \end{aligned} \quad (9)$$

$$u_i[n] = u_i[n-1] + \frac{K_p}{T_i} \cdot T_a \cdot e[n]$$

Figure 8 shows the dynamic response of the PI controller for a step in average current reference. The current $i(t)$ corresponds to the current in the load, with a pulse density of 5/40. It is observed that the response is slow compared to the switching frequency of the system, which is 3 kHz. This is not a problem, because the saturation of the transformer is also a slow process [11].

V. EXPERIMENTAL RESULTS

The system shown in Fig. 9 was implemented using four IGBT embedded on the smart power module IRAMX20UPA. The PI controller, the instantaneous current controller and the PDM modulator were implemented in the microcontroller TMS320F28335. The parameters of the transformer and the ozone cell were determined as suggested in Session III and shown in table 1.

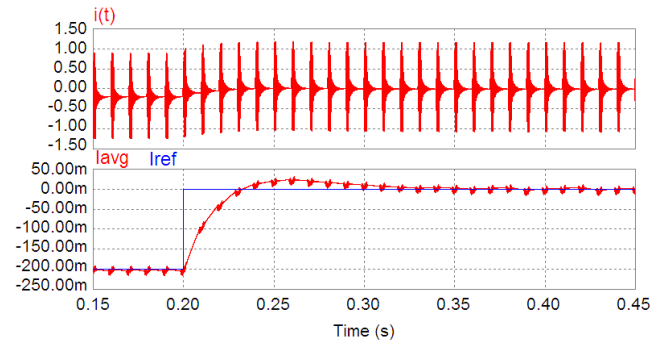


Fig. 8. Response to a step in reference of average current.

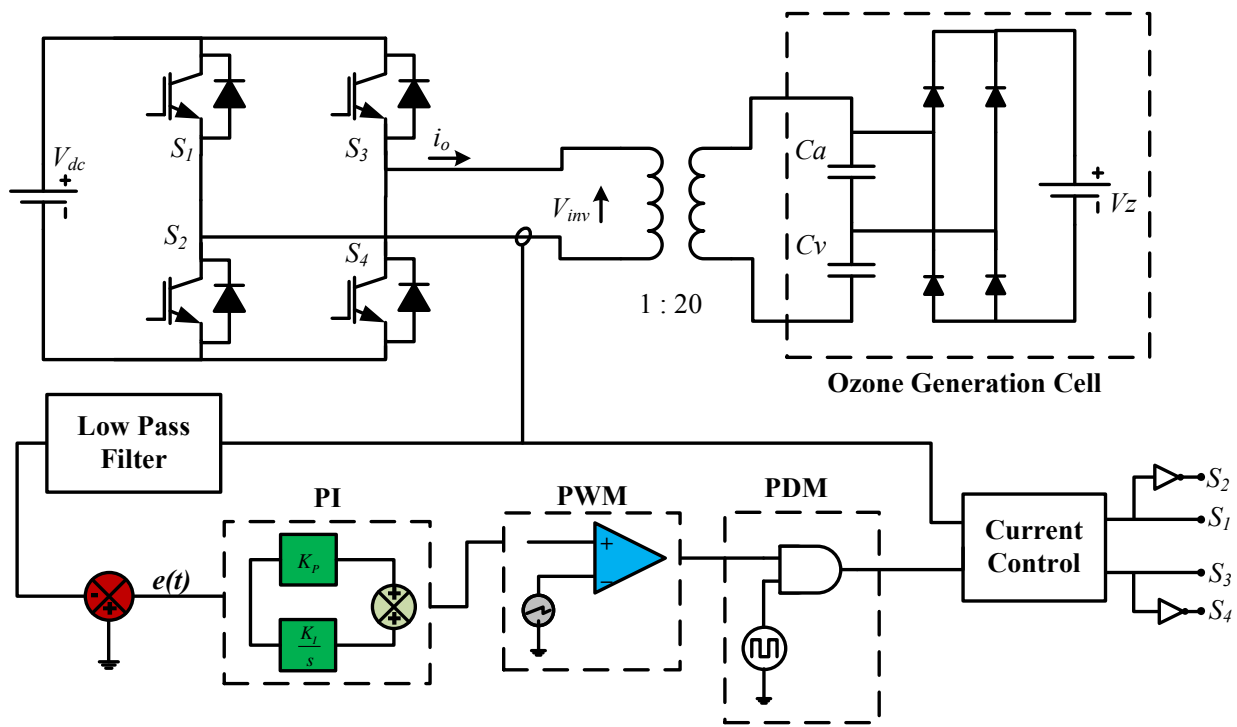


Fig. 9. Overview of the power converter and control system.

TABLE I
ESTIMATED PARAMETER OF THE TRANSFORMER CONNECTED TO OZONE CELL

L_d [mH]	L_m [mH]	C_{eq} [nF]	R_s [k Ω]	R_p [k Ω]
32	390	180	3.6	20

Through the equation of the impedance of the transformer, and respective parameters, it is possible to get the frequency response of input impedance, as shown in Fig. 10. The parallel resonance frequency is approximately 0.6 kHz and the series resonance of 2.2 kHz. The switching frequency is chosen to be 2.4 kHz, because it is of interest to work in the inductive region, and due to the high voltage gain obtained near the series resonance.

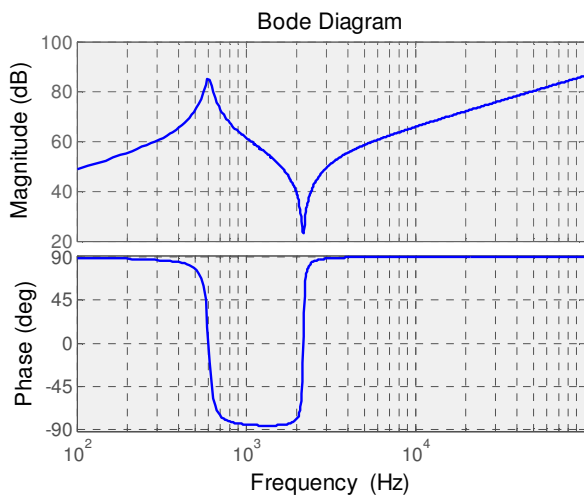


Fig. 10. Bode diagram of the whole transformer plus load.

Moreover, to achieve soft switching of the switches, it is necessary to operate in a frequency above the series resonance. Thus, when the switches are activated, the current is flowing through the diodes, providing conduction under zero-current. At the end of conduction interval, the current is flowing through the transistor. With the help of the parasitic capacitances of the IGBTs, or additional external capacitance, it is possible to realize zero-voltage commutation.

To verify the dynamic behavior of the control system, especially the PI controller, it is forced an average level in the load current of approximately 200 mA. When the step occurs, the controller starts to target zero average current. The response to this reference step can be seen in Fig. 11. The controller has a response time of about 1s. Note also the first order behavior, due to the low value proportional gain chosen.

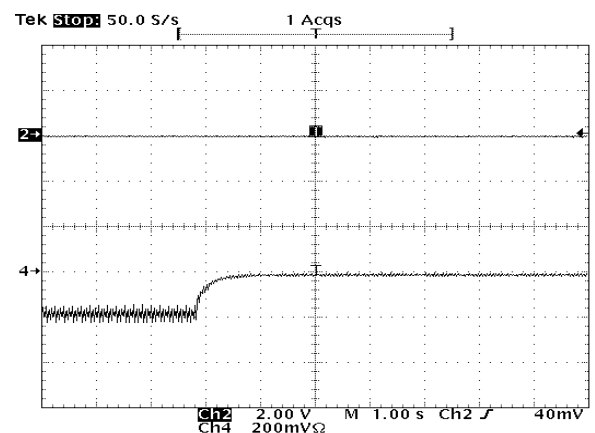


Fig. 11. Response of PI to a step in the reference. Ch2 shows the average output current.

Figure 12 shows the current and voltage waveforms at the inverter output, for a pulse density of 27/40. The DC link voltage is 160 V. It is clear the transformer goes to saturation, what is indicated by the increasing load current negative peaks. Figure 13 repeats these waveforms, but now with the active controls.

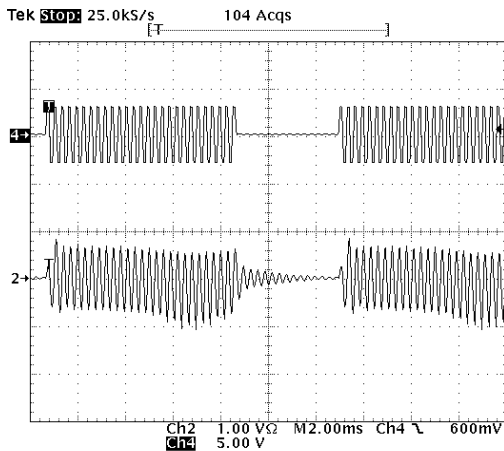


Fig.12. Voltage (Ch4) and current (Ch2) in the inverter output (without the application of control).

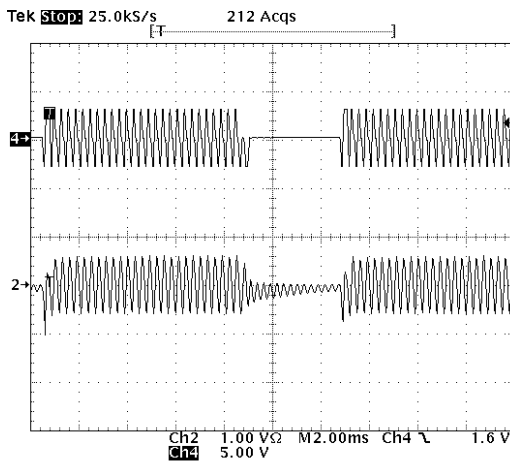


Fig. 13. Voltage(Ch4) and current (Ch2) in the inverter output (with controls acting).

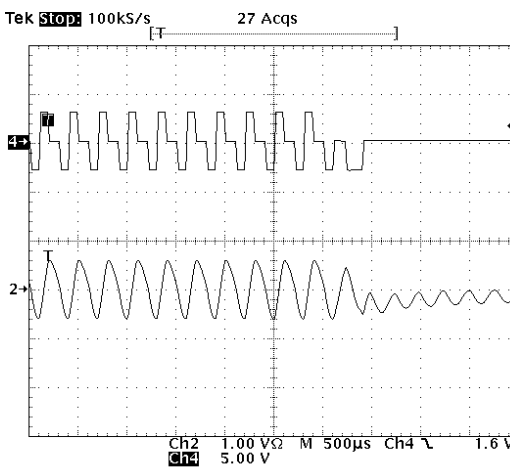


Fig. 14. Detailed view of voltage (Ch4) and current (Ch2) with the application of controls

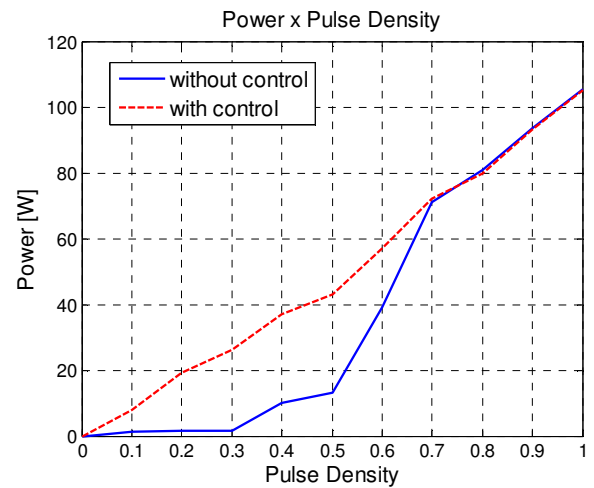


Fig. 15. Relationship between pulse density and inverter output power for controlled and non-controlled version.

Note that the current waveform has a flatter profile, without the variation caused by saturation of the transformer.

A detailed view of these waveforms shows the performance of controls, as displayed in Figure 14. The positive semi-cycles of voltage pulses would be wider than the negative ones. However, the positive pulses are finished when the current reaches the ceiling, keeping the average level of current close to zero.

Figure 15 indicates the relationship between pulse density and output power of the inverter, obtained experimentally. The solid line was obtained by open loop operation (without current neither voltage control). On the other hand, the dashed line, obtained applying the proposed control techniques shows a quite linear characteristic.

Figure 16 shows the relationship between pulse density and efficiency of the electronic converter. The measurements were taken with WT300 Precision Power Analyzer. The dashed line presents the values for closed loop operation with the controls techniques, while the solid line was obtained without applying controls.

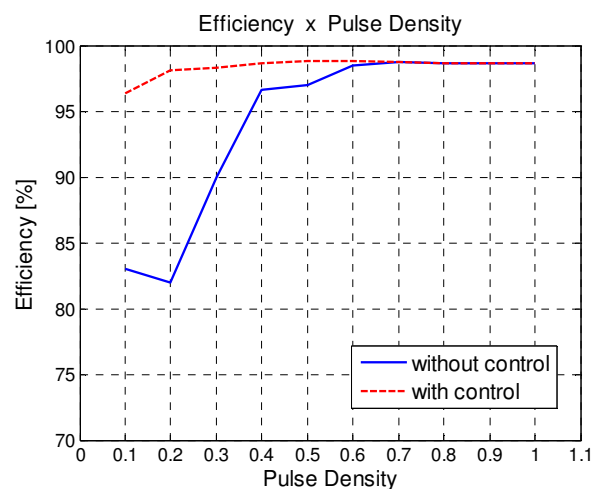


Fig. 16. Relationship between pulse density and inverter efficiency for controlled and non-controlled version.

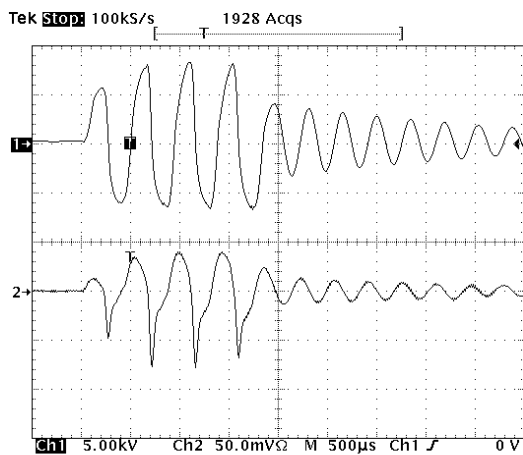


Fig. 17. Voltage(Ch1) and current (Ch2)) in the secondary side of transformer (without applying controls).

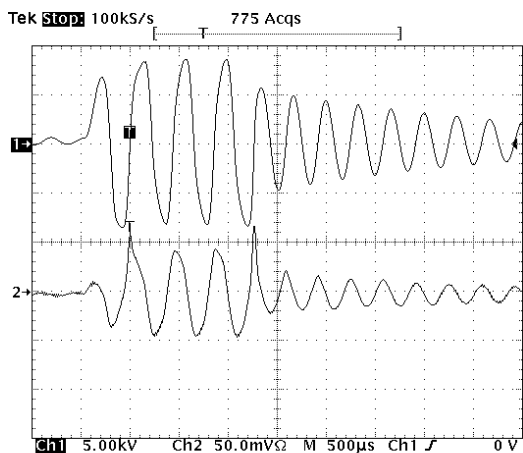


Fig. 18. Voltage(Ch1) and current (Ch2)) in the secondary side of transformer (applying controls).

For high pulse densities, the results obtained with or without the controls techniques are basically the same. In both cases the converter was operated with fixed frequency of 2.4 kHz and DC link voltage of 170 V. The maximum inverter output power and efficiency was respectively 108 W and 98%. On the other hand, for low pulse densities the proposed controls techniques improved both the efficiency and the inverter output power, since the saturation of the transformer is controlled.

Figure 17 shows the high voltage waveform for a pulse density of 4/20. Note the peak present in the current due to the transformer saturation. This is the main cause of the low efficiency and low inverter output power presented above. As the pulse density decrease, this effect gets worst. Fig. 18 shows the same waveform, but now applying the control techniques, minimizing and controlling the transformer saturation.

VI. CONCLUSIONS

This paper has proposed a technique to avoid the saturation of transformer of high frequency and high voltage converter for ozone generation by electrostatic discharge, using a

voltage fed inverter. The resonant converter operates with constant switching frequency, above the series resonance frequency, in which range it achieves high voltage gain and soft-switching.

The saturation of the transformer is avoided by a rapid limitation of the peak current and a control loop that acts on the average current and on the command pulses in order to maintain zero average voltage and current. The control prevents the current to reach values that would compromise the safe operation of the inverter. Moreover, the average value control has the function of correcting the unbalance caused by possible asymmetries in the command of the power switches used in the bridge inverter.

The output power of the converter was regulated through the pulse density modulation. Together with the saturation control technique it guarantees a linear power variation, without changes in the peak voltage value of the ozone cell.

ACKNOWLEDGMENT

This work is supported by the Foundations FAPESP, CNPq and CAPES. The authors thank Panozon Ambiental for the ozonizer cells and general technical support.

REFERENCES

- [1]. G. S. Sperandio, J. A. Pomilio: "High-efficiency, high-frequency inverter for silent discharge load", Proc. of 9th Brazilian Power Electronics Conference – COBEP 2007, Blumenau, Brazil, 30/9 to 4/10/2007, pp. 895-890.
- [2]. O. Koudriavtsev, S. Wang, Y. Konishi, and M. Nakaoka, "A novel pulse-density-modulated high-frequency inverter for silent-discharge-type ozonizer", IEEE Transactions on Industry Applications, vol. 38, No 2, March/April 2002.
- [3]. J. Alonso, J. Garcia, A. Calleja, J. Ribas, and J. Cardesin, "Analysis, design, and experimentation of a high-voltage power supply for ozone generation based on current-fed parallel-resonant push-pull inverter", IEEE Transactions on Industry Applications, vol. 41, no. 5, pp. 1364–1372, Sept.-Oct. 2005.
- [4]. H. Yushui, W. Liqiao, X. Yu and Z. Zhongchao, "Load resonant type power supply of the ozonizer based on a closed-loop control strategy", IEE 2004.
- [5]. H. W. Ahn , H. G. Joo, and M. J.Youn, "Improved pulse density modulation for high-frequency series resonant inverter with transformer-coupled load", Int. J. Electronics, 1998, Vol. 84, No. 1, 1997.
- [6]. J. Alonso, M. Valdes, A. Calleja, J. Ribas, and J. Losada, "High Frequency Testing and Modeling of Silent Discharge Ozone Generators" Ozone Science & Engineering Journal, Vol. 25, No. 5, 2003, pp. 1296-1204.
- [7]. J. Alonso, J. Garcia, A. Calleja, J. Ribas, and J. Cardesin, "Analysis, design, and experimentation of a high-voltage power supply for ozone generation based on current-fed parallel-resonant push-pull inverter", Industry Applications, IEEE Transactions on, vol. 41, no. 5, pp. 1364–1372, Sept.-Oct. 2005.
- [8]. S. Wang, M. Nakaoka, and Y. Konishi, "DSP-based PDM and PWM type voltage-fed load-resonant inverter with high-voltage transformer for silent discharge ozonizer", in Power Electronics Specialists Conference, 1998. PESC 98 Record. 29th Annual IEEE, vol. 1, 17-22 May 1998, pp. 159–164 vol.1.
- [9]. K. Ogata. Engenharia de controle moderno, 4ª edição, Prentice-Hall, 2003.
- [10]. P. Mattavelli and S. Buso. Digital control in power electronics. 1st ed. Morgan & Claypool Publishers.
- [11]. L. Bolduc, A. Gaudreau, A. Dutil, "Saturation time of transformers under dc excitation", Elsevier Electric Power Systems Research Vol. 56, 2000, pp. 95–102.